Available online at www.sciencedirect.com
ScienceDirect
Optics Communications 281 (2008) 1189–1196
OPTICS COMMUNICATIONS
www.elsevier.com/locate/optcom

A crossed optical cavities apparatus for a precision test of the isotropy of light propagation

Ch. Eisele *, M. Okhapkin [1], A.Yu. Nevsky, S. Schiller

Institut für Experimentalphysik, Heinrich-Heine-Universität Düsseldorf, 40225 Düsseldorf, Germany

Received 14 May 2007; received in revised form 16 October 2007; accepted 17 October 2007

Abstract

A novel apparatus for a sensitive test of the independence of the speed of optical waves from the propagation direction has been developed. It employs a monolithic ULE glass structure containing two orthogonal, crossing Fabry–Perot cavities which enable common mode rejection of certain disturbances. Highly accurate locking and cavity frequency read-out are achieved using laser frequency modulation at audio frequencies. Several systematic effects were characterized. Without rotation the root Allan variance (RAV) of the beat frequency reaches a minimum of 0.5 Hz (2×10^{-15}) close to the thermal noise floor of the cavities. The performance of the apparatus under rotation is demonstrated by determining with improved accuracy one parameter of the standard model extension test theory, $(\tilde{\kappa}_{e-})^{ZZ} = (-1.0 \pm 2.3) \times 10^{-15}$, under simplifying assumptions.

PACS: 03.30.+p; 06.30.Ft; 42.60.Da

1. Introduction

The independence of the speed c of electromagnetic waves in vacuum from the direction of propagation, a postulate of special relativity, has been verified with steadily increasing accuracy since the historic experiment of Michelson and Morley [1] and is today one of the most accurately tested symmetries of nature [2–8]. The upper limit for a hypothetical anisotropy of c furnished by the most recent experiments is, within a theoretical framework developed by Mansouri and Sexl [9], several parts in 10^{16}. Within the standard model extension (SME) [10–13], an alternative framework, upper bounds for a number of Lorentz invariance violation parameters have been determined [3–8].

Briefly, a test of this symmetry requires preparation of at least one optical path that is very stable on time scales lying between tens of seconds (for an experiment in which the apparatus is actively rotated) to half a day (for a non-rotating experiment), as well as a very precise means of measuring changes of its length relative to a reference.

Recent experiments in the optical spectral range were performed using a pair of orthogonal Fabry–Perot cavities as ''rulers''. Lasers were frequency-stabilized to the respective cavities. The search for a hypothetical anisotropy of the speed of light was done by analyzing the beat signal between the lasers as a function of the cavities' orientation in space.

Here we present the characterization of a novel apparatus that represents a significant improvement on previous ones in terms of sensitivity. The main features of the present apparatus are a monolithic structure containing two orthogonal reference cavities [14] and the use of ultra-low-expansion coefficient glass (ULE), allowing convenient operation of the setup at room temperature.

* Corresponding author. Fax: +49 0211 81 13116.
E-mail addresses: christian.eisele@uni-duesseldorf.de (Ch. Eisele), alexander.nevsky@uni-duesseldorf.de (A.Yu. Nevsky).
[1] Permanent address: Institute for Laser Physics, Novosibrisk, Russia.

0030-4018/$ - see front matter © 2007 Elsevier B.V. All rights reserved.
doi:10.1016/j.optcom.2007.10.071

2. Experimental apparatus

2.1. Overview

A schematic of the apparatus is presented in Fig. 1. Its central part is a monolithic ULE block (see Fig. 2) of size $84 \times 84 \times 35$ mm, containing two orthogonally embedded cavities. These cavities are formed by high-reflection mirrors (Research Electro-Optics, Inc.) for the center wavelength of 1064 nm ($\nu_0 = 282$ THz), optically contacted to the sides of the block. In the cavity block, the light propagates inside cylindrical holes (8 mm diameter). The cavities exhibit a finesse of 190 000 and an optical throughput of 16%. A small hole drilled perpendicularly to one of the cavities allows pumping out the cavities. The rigid monolithic construction of the block ensures a strong common mode rejection of thermal and mechanical disturbances of the frequency difference between the cavities, i.e. the beat frequency $\nu_b = \nu_2 - \nu_1$ between the two cavities is less sensitive to certain perturbations than the absolute frequency of an individual cavity.

For acoustic and thermal isolation from the environment the cavity block is mounted inside a vacuum chamber ($p \approx 10^{-7}$ mbar) made from stainless steel. The vacuum chamber is placed in a temperature and acoustic isolation box with entrance windows for the laser radiation. The temperature inside the box is stabilized at about 30 °C using a heating wire, wrapped around the vacuum chamber.

In order to improve the short-term frequency stability of the cavities, the setup is placed on active vibration isolation supports (AVI, model AVI-350 M, HWL-Scientific), which strongly reduces frequency jitter of the cavity caused by mechanical vibrations [15]. A further reduction of the vibration sensitivity of the beat frequency as compared to the absolute frequency is obtained due to common mode rejection, since the orthogonal cavities are similarly disturbed by vertical acceleration noise.

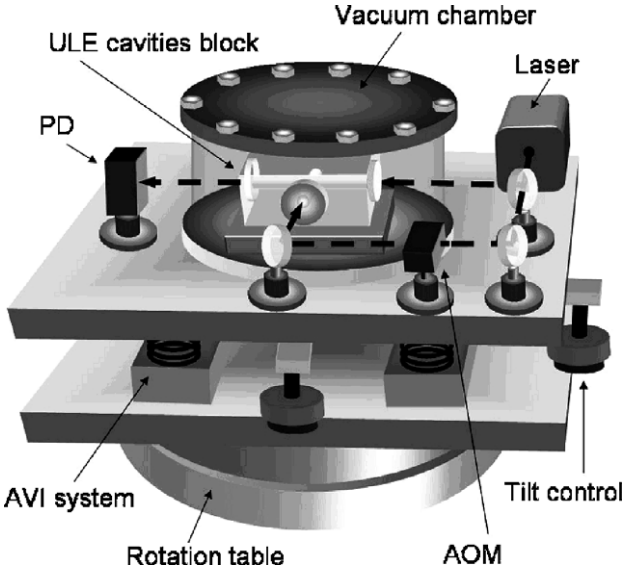

Fig. 1. Schematic of the experimental setup (without housing). AVI – active vibration isolation system, AOM – acousto-optical modulator, PD – photo detector. The size of the two breadboards is 90×90 cm.

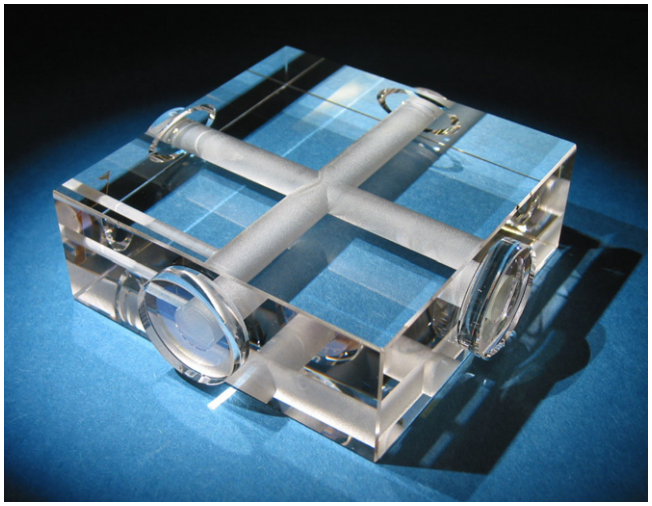

Fig. 2. The dual-cavity ULE block.

The experimental apparatus (containing the Nd:YAG laser, modulators, optical components, AVI) is placed on a motorized rotation stage that rests on a granite block. The complete setup is operated inside a large box ($1.5 \times 1.5 \times 2.5$ m), the sides of which are made of multilayered acoustic and thermal isolation materials. The top of the box is made of aluminum plates which are temperature-stabilized using a large number of thermo-electric coolers (TECs). This construction allows isolating the whole apparatus against acoustic noise and air currents, as well as providing an additional temperature stabilization stage for the cavities and the setup in general.

2.2. Thermal properties of the cavities

A particular property of the ULE material is a zero thermal expansion coefficient (CTE) at a temperature usually between 10 and 35 °C, as declared by the manufacturer. Operating the ULE resonators at this particular temperature minimizes the influence of temperature changes on their resonance frequencies. The temperature of the zero CTE was determined in the following way. Two similar ULE blocks (A and B), each containing two orthogonal cavities, were mounted inside the same vacuum chamber. The vacuum chamber was placed inside a box made of 8 mm thick aluminum plates. Each plate was independently temperature-stabilized using Peltier elements (TECs). In order to reduce the temperature gradients between the sides of the box, the temperature sensors (AD590), fixed on each aluminum plate, were precisely calibrated. To provide an efficient heat exchange between the hot and cold sides of the TECs, each of them was connected to heat sinks with a large surface. These heat sinks on each side of the aluminum box formed another closed chamber, which also served as an additional temperature and acoustic isolator.

For measuring the cavity frequencies as a function of the block temperature, an iodine-stabilized Nd:YAG laser at 1064 nm with intra-cavity frequency doubling was used [16]. The laser was frequency-stabilized to a hyperfine-structure (HFS) component of molecular iodine using Doppler-free modulation transfer spectroscopy. The stabilized 1064 nm wave was split into four parts and resonantly coupled into each cavity after being frequency-shifted using acousto-optical modulators (AOM). Thus, a variation of the resonance frequency of a cavity with respect to the iodine transition was obtained directly from the AOM frequency.

The Nd:YAG laser frequency was scanned with an amplitude of several MHz at a low frequency of about 10 Hz and the cavity frequencies were manually superposed with the iodine transitions by observing simultaneously all the signals on a storage oscilloscope. The width of the iodine saturation absorption resonances in our setup is about 500 kHz and the absolute accuracy is of the order of 10 kHz. The overall measurement error is estimated to be about 50 kHz.

The result of the measurement is shown in Fig. 3, which displays $\alpha = (\mathrm{d}\nu/\mathrm{d}T)/\nu_0$ for each cavity. Due to the large thermal time constant of the ULE blocks inside the vacuum chamber (about 5 h), each data point was measured with an interval of 24 h in order to ensure steady-state conditions. The temperatures of zero CTE were found to be slightly different for all cavities. This difference prevents simultaneous operation of the cavities of either block at zero CTE. The differential expansion coefficients $(\mathrm{d}\nu_b/\mathrm{d}T)/\nu_0 = (\alpha_2 - \alpha_1)$ are $6 \times 10^{-10}\,\mathrm{K}^{-1}$ for block B and $1.1 \times 10^{-9}\,\mathrm{K}^{-1}$ for block A, as evaluated from Fig. 3. These values depend only weakly on the block temperature.

As a test of the common mode rejection of the temperature fluctuations for the two cavities of the same block, the frequency of one of the ULE cavities of block B was compared with that of an optical sapphire resonator operated at cryogenic temperature [17,18]. In order to reduce the error due to any residual drift of the sapphire resonator, the temperature stabilization of the ULE block was switched off, leading to a large frequency drift of the individual ULE-cavities $\mathrm{d}\nu_i/\mathrm{d}t \approx 70$–$80$ Hz/s.

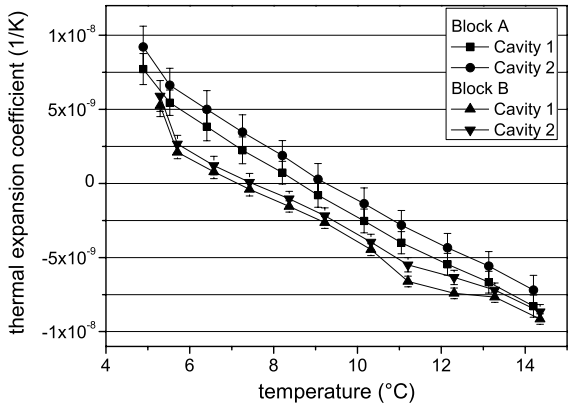

Fig. 3. Temperature dependence of the thermal expansion coefficients of the ULE cavities.

Later the drift of the sapphire resonators was measured with respect to a femtosecond frequency comb to be about 0.01 Hz/s, confirming the negligible contribution to the measurement error.

The differential drift rate (beat signal drift rate $\mathrm{d}\nu_b/\mathrm{d}t = \mathrm{d}\nu_2/\mathrm{d}t - \mathrm{d}\nu_1/\mathrm{d}t$) was measured to be 1.4 Hz/s, corresponding to a suppression factor $K_S = |(\mathrm{d}\nu_i/\mathrm{d}t)/(\mathrm{d}\nu_b/\mathrm{d}t)| = 53$ with respect to an individual cavity due to common mode rejection. This value is in good agreement with an extrapolation of the data shown in Fig. 3 to the temperature at which this measurement was performed (approx. 30 °C). All further measurements are performed at this temperature, chosen close to the temperature value in the shielding box, so as to minimize the power consumption of the system.

Note that since $(\mathrm{d}\nu_b/\mathrm{d}T)/\nu_0$ is, with good approximation, constant in the considered temperature range (see Fig. 3), the suppression factor K_S can have values ranging from 0 (at a temperature for which an individual cavity has zero CTE) to large values, for a sufficiently large offset temperature.

2.3. Locking scheme

A schematic of the lock system is shown in Fig. 4. It consists of a prestabilization lock and a high-accuracy read-out of the cavity frequency difference using low-frequency modulation locks.

The laser source is a Nd:YAG laser at 1064 nm (Innolight Mephisto). It is tunable both via the resonator temperature by means of a TEC element, or by using a piezoelectric (PZT) actuator glued to the Nd:YAG crystal that changes the resonator length due to the applied stress. The laser radiation is split into three main beams using AOMs. A first beam (beam 3 in Fig. 4) is used for prestabilization of the laser frequency. It is obtained by a double pass through AOM 3 leading to a 760 MHz frequency shift, and is then mode-matched to the TEM_{01} mode of one of the ULE cavities. The laser frequency is locked to this mode using the Pound–Drever–Hall technique. The laser radiation is therefor phase modulated by the electro-optical modulator (EOM) at a frequency of 2.05 MHz. The frequency servo consists of a fast and a slow loop. The fast stabilization uses the PZT actuator. The bandwidth of this lock is about 30 kHz, limited by the strong mechanical resonances of the actuator. The slow loop (bandwidth 0.1 Hz) is used to control the temperature of the laser crystal. This frequency stabilization system keeps the laser in lock uninterruptedly for many days.

For the accurate read-out of the cavity frequencies, beams 1 and 2 are used. AOM 1 shifts part of the laser beam by approx. 128 MHz to generate beam 1, while AOM 2 generates beam 2, which is frequency-shifted by about −119 MHz. Beam 2 is led into the same cavity as

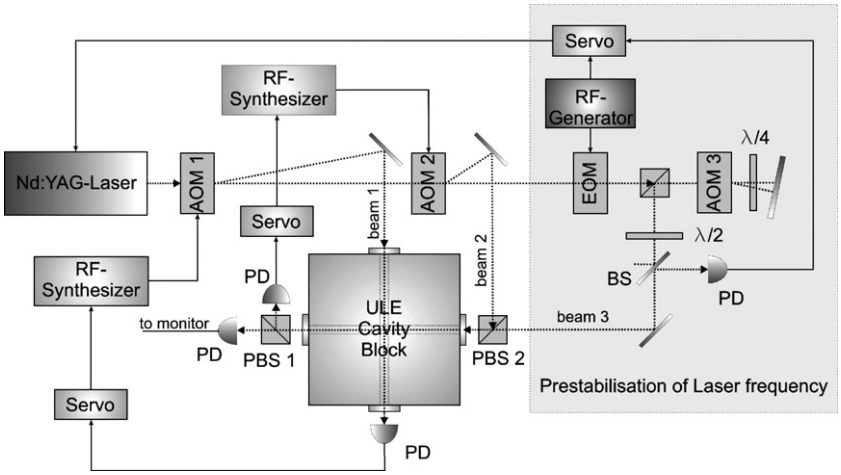

Fig. 4. Scheme of the laser frequency stabilization. PD – photodiode, BS – beamsplitter, EOM – electrooptical modulator, AOM – acousto-optical modulator, and PBS – polarising beamsplitter.

the prestabilization beam 3, but exciting the TEM_{00} mode. The polarization of this beam is orthogonal to the polarization of beam 3 locked to the TEM_{01} mode. Beam 1 is coupled to the TEM_{00} mode of the orthogonal cavity.

Beams 1 and 2 are independently locked to the respective cavities. The locks are based on synchronous detection of intensity modulation of the light transmitted through the cavities. Beam 1 is therefore frequency modulated by AOM 1 at 3.4 kHz, while beam 2 is modulated at 4.08 kHz by AOM 2. The detection is performed at the respective modulation frequencies. The generated error signals are appropriately amplified and then applied to the FM inputs of the RF synthesizers, driving the corresponding AOMs. The bandwidth of the loops is about 500 Hz. The use of separated locks, narrow locking bandwidth, detection of the transmitted signal (which increases the contrast of the signal) and the low frequency of the probe modulation allow reducing the influence of different parasitic effects, such as spurious interferences and residual amplitude modulation (RAM).

2.4. Systematics

We have investigated a number of potentially disturbing effects by measuring the response of each cavity on these perturbations.

The effect of RAM is similar for both cavities due to the almost identical realization of the locking system and is below 0.02 Hz, as determined from the open loop error signal of the locking system, resulting in a contribution to the frequency instability of few parts in 10^{17} (see Fig. 5) at the timescale of interest (tens of seconds).

A second effect is cavity heating by the interrogating beams, leading to a power-dependent cavity frequency shift. This effect was measured to be on the order of 3 Hz/μW. To minimize its influence, the circulating power is stabilized by detecting the radiation transmitted through the cavity and controlling the RF power applied to the AOMs. The bandwidth of the power locking system is about 2 kHz.

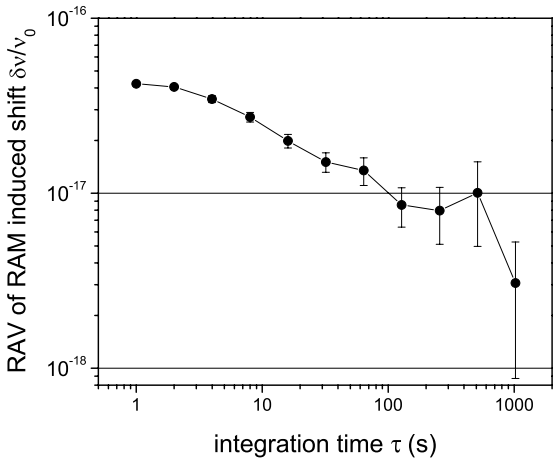

Fig. 5. Inferred frequency instability (for a single cavity) induced by drift of the lock offset due to residual amplitude modulation.

The result of the power stabilization is presented in Fig. 6, showing the relative root Allan variance of the residual power fluctuations multiplied by the measured power sensitivity. The resulting effect on the beat frequency is not higher than 3×10^{-17} for integration times above 20 s. The larger instability found for cavity 2 around $\tau = 70$ s is attributed to a crosstalk between the prestabilization and the fine lock system for the same cavity, since the beams cannot be perfectly separated at PBS 1 due to imperfect polarization. Another possible contribution is a crosstalk between the power stabilization systems controlling AOM 1 and AOM 2.

Another important disturbance is tilt of the experimental setup. It leads to a deformation of the cavity block and, as a result, changes the beat frequency. Variations in tilt are caused by temperature variations, as well as by active rotation. The tilt sensitivities for the two cavities of the ULE block were measured to be 0.045 Hz/μrad and 0.135 Hz/

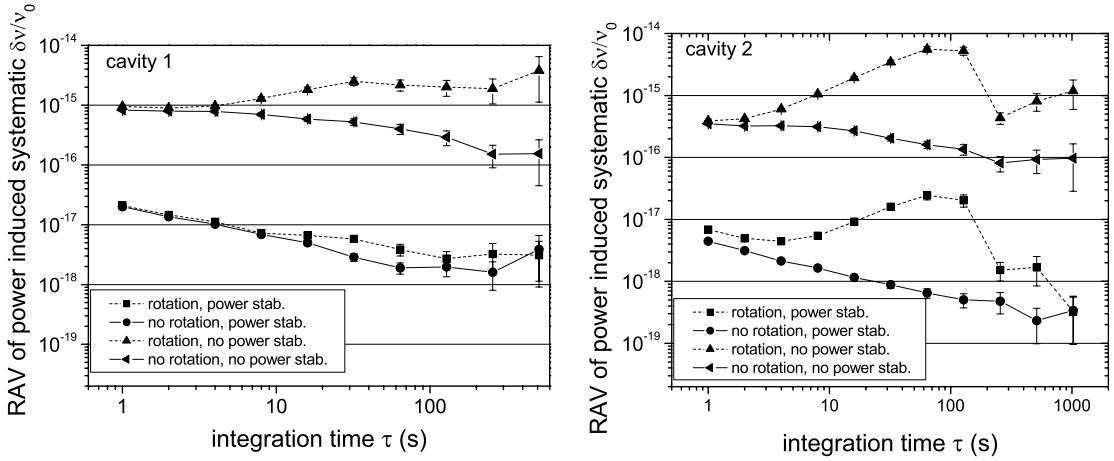

Fig. 6. Inferred instability of the cavity resonance frequency difference ν_b caused by residual laser power fluctuations present in cavity 1 (left) and cavity 2 (right). Shown are the behaviours for all combinations of rotation on/off and power stabilization on/off.

μrad, respectively, where the tilts were applied in vertical planes containing the respective cavity axis. In order to actively stabilize the tilt we implemented a digital control that uses two electromechanical actuators (EMA), attached on the orthogonal sides of the experimental breadboard, and a two-axis tilt sensor (Applied Geomechanics model 755-1150, angular resolution 1 μrad) to obtain the error signal. The AVI system supporting the setup operates in the frequency range of about 1–100 Hz. At lower frequencies its spring suspension has a unity transmission coefficient. The height of the AVI supports can be altered by the EMAs, allowing tilts in the range of several hundred μrad without degrading the AVI performance. The time constants of the two regulation systems were chosen appropriately in order to prevent a cross coupling.

We determined the root Allan variance of the residual tilt instability of the stabilized system for the cases of apparatus rotation (240 s period) and rest. The results were multiplied by the measured tilt sensitivities and are displayed in Fig. 7. The rotation table was a standard ball bearing rotation table. It exhibits a rather large intrinsic modulation of the rotation axis orientation of tens of μrad. This results in a bulge in the RAV when the tilt stabilization is off, shown in Fig. 7 for both axes. The tilt stabilizer reduces this by a factor of approx. 10 at $\tau = 60$ s to a 1 μrad amplitude. The residual systematic effect on the beat frequency (RAV) is at a level of 0.03 Hz for the x-axis and 0.15 Hz for the y-axis at an integration time of a quarter of the rotation period, corresponding to a fractional effect of 1.2×10^{-16} and 5.2×10^{-16}, respectively (see Fig. 7). The actual influence can be reduced further if a correction for the uncompensated tilt is applied in the data analysis [5].

We emphasize that these results are obtained with a low-performance table. High-performance rotation tables with air bearings can exhibit axis wobble as low as a few μrad, which can be further reduced by the tilt control system. With such table specifications we expect the influence of the residual tilt instability to be approx. one order of magnitude lower than the above values.

Fig. 8 shows the root Allan variance of the beat frequency. Linear and quadratic drifts have been removed, since these contributions do not influence the later

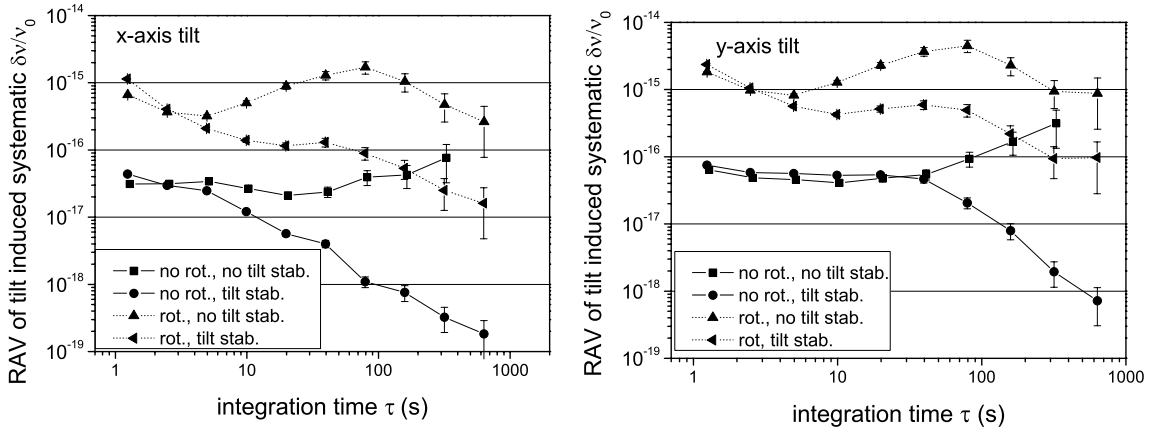

Fig. 7. Inferred root Allan variance of the cavity resonance frequency difference ν_b caused by table tilt variations around different axes (left: x-axis, right: y-axis). Dashed lines: under rotation of the setup with a period of 240 s and solid lines: without rotation of the setup.

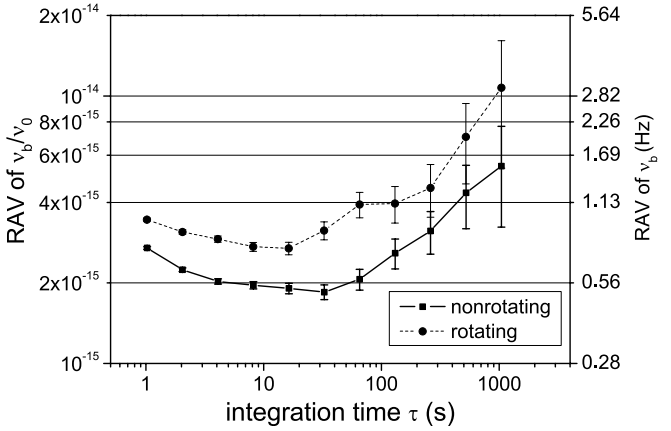

Fig. 8. Root Allan variance of the beat signal between the two laser waves 1 and 2, locked to the orthogonal cavities of the same ULE block. Linear and quadratic drifts are removed, no decorrelation of residual systematics is performed. The bump in the dashed line at 60–200 s is due to rotation (240 s period).

evaluation of the data. For the stationary setup, the residual instability is about 0.8 Hz at 1 s and has a minimum of 0.5 Hz (1.9×10^{-15}) at 32 s. The cavity thermal noise leads to a constant contribution to the Allan variance [19]. An estimate can be given using the typical material properties quoted in [19] for ULE. Since the thermal noise is dominated by the mirror contribution, the unusual shape of the cavity block is of lesser importance. The thermal noise contribution is estimated as 0.4 Hz. Considering the uncertainty of this estimate, we conclude that the performance of our system at short integration times is close to the thermal noise limit.

For the rotating setup the residual instability of the beat frequency reaches a minimum of 0.76 Hz (2.7×10^{-15}) at 16 s integration time, about 50% higher than without rotation. In view of the level of systematics described above, this increased instability appears to be due to other noise sources, probably a combination of residual vibrations, acoustics from inside the tower (vents, etc.), temperature drifts and gradients, electrical pickups in the rotary feedthrough and beam pointing instability.

2.5. Detection sensitivity

The maximum detection sensitivity of the setup can be determined by performing measurements with a non-rotating setup. Of particular relevance is then the noise occurring at integration times corresponding to one-quarter the planned rotation period since a violation of the isotropy of light propagation would appear as a signal with period equal or nearly equal to half the rotation period.

A typical measurement of the beat signal between the two waves locked to the orthogonal cavities of the ULE block is shown in Fig. 9 for the non-rotating case. Linear (about 0.1 Hz/s) and quadratic drifts of the beat signal were subtracted from the original dataset, which was then split in intervals of $T = 2\pi/\Omega = 40$ s length (planned rotation period for a future air bearing table). Finally, the data of all intervals were averaged arithmetically. As Fig. 9a shows, averaging reduces the noise substantially. A fit (see Fig. 9b) of a hypothetical signal gives an estimate for the detectable signal in absence of systematic effects connected to rotation. For a dataset of approx. 17 h length, a signal with amplitude exceeding a few tens of mHz ($\Delta\nu/\nu_0 \approx 4 \times 10^{-17}$) is detectable.

As an alternative evaluation we have taken the same beat data record and added to it a coherent signal $\Delta\nu = 2C\nu_0\cos(2\Omega t) + 2B\nu_0\sin(2\Omega t)$, with arbitrarily chosen amplitudes $2C\nu_0 = 0.1$ Hz, $2B\nu_0 = 0.2$ Hz. This ansatz comes from the theoretical framework used to interpret the results of the experiment [9]. We analyzed the data by again dividing the record into intervals of one rotation period, to each of which we fitted simultaneously harmonic modulations of 20 and 40 s period plus a linear beat frequency drift. The histograms of $2C\nu_0$ and $2B\nu_0$ are shown in Fig. 10. The mean values and their statistical errors are (0.113 ± 0.008) Hz and (0.214 ± 0.010) Hz, respectively. Thus, the simulated modulation is recovered with good fidelity. The error of the vector amplitude is about 0.01 Hz, in relative units 3.5×10^{-17}.

Thus, we find that the present apparatus exhibits a potential sensitivity at a level of several parts in 10^{17} for an integration time of about 1 day. In the absence of systematic effects this would be the maximum achievable sensitivity, and, with sufficient long-term stability of the apparatus, the sensitivity would improve by extending the measurement duration.

3. Isotropy test

We have performed measurements under rotation with $T_r = 240$ s rotation period. At this period a compromise between short duration and low vibration of the rotation table was found.

Fig. 11 shows the modulation amplitudes $2C\nu_0$ and $2B\nu_0$ of a large number of rotations (3050, for a total duration of 8.6 days), taken in five sets spread over 45 days. Tilt modulation systematics at one-half the rotation period corresponded to values between 0.4 and 2 Hz, higher than the lowest achievable ones (described above), since no effort was made to adjust the granite plate on a regular basis. In the data analysis both tilt and power modulation corrections were implemented.

The resulting corrected $2C\nu_0$ and $2B\nu_0$ data is still affected by systematics, as can be seen from the presence of trends in the respective time series. The origin is unidentified so far. The standard deviation of the data for $2C$ is 2.4×10^{-15}.

We can determine one coefficient of the SME test theory, $(\tilde{\kappa}_{e-})^{ZZ}$. The other SME coefficients relevant for modeling a Michelson–Morley experiment in the photon sector, the remaining elements of the matrices (κ_{e-}), and the elements of $\beta(\tilde{\kappa}_{o+})$ (βc is the speed of the solar system relative to the microwave background), have recently been deter-

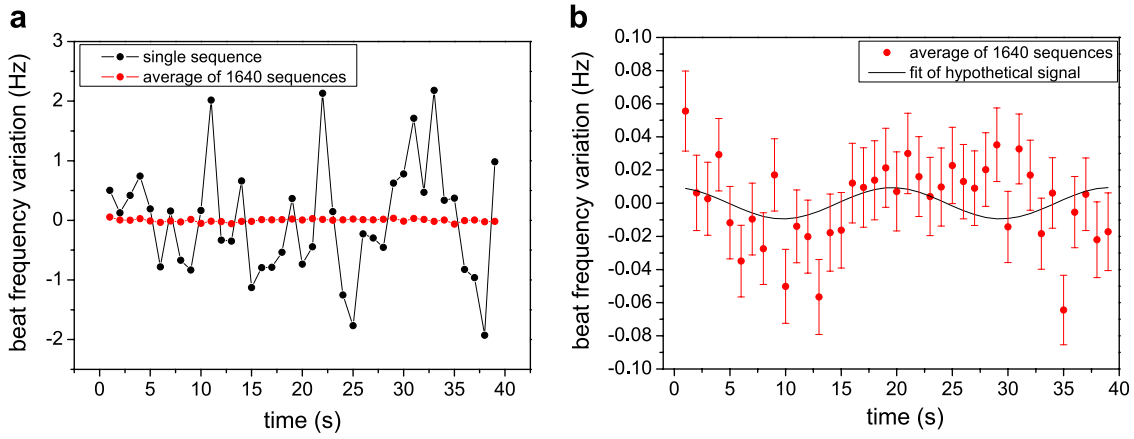

Fig. 9. (a) Beat signal between the two orthogonal cavities (non-rotating): single interval of 40 s length and the average of 1640 such intervals (from a 17 h long dataset). (b) On an extended scale, the average from (a) with statistical errors and the fit of a hypothetical modulation $D \cdot \sin(2\Omega t + \Phi)$.

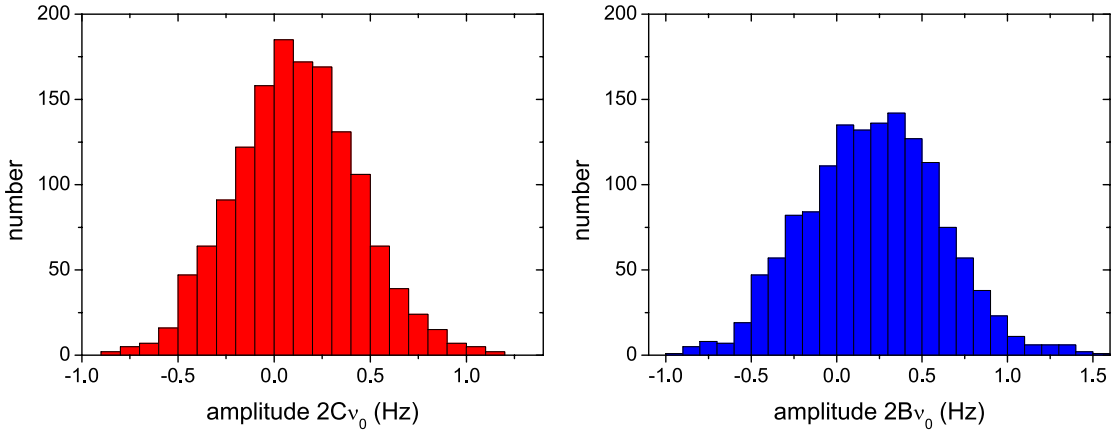

Fig. 10. Statistics of a simulated isotropy violation signal, appearing as a nonzero average for the two amplitudes $2Cv_0$ and $2Bv_0$. A coherent signal was added to the dataset (same dataset as used for Fig. 9) before the analysis.

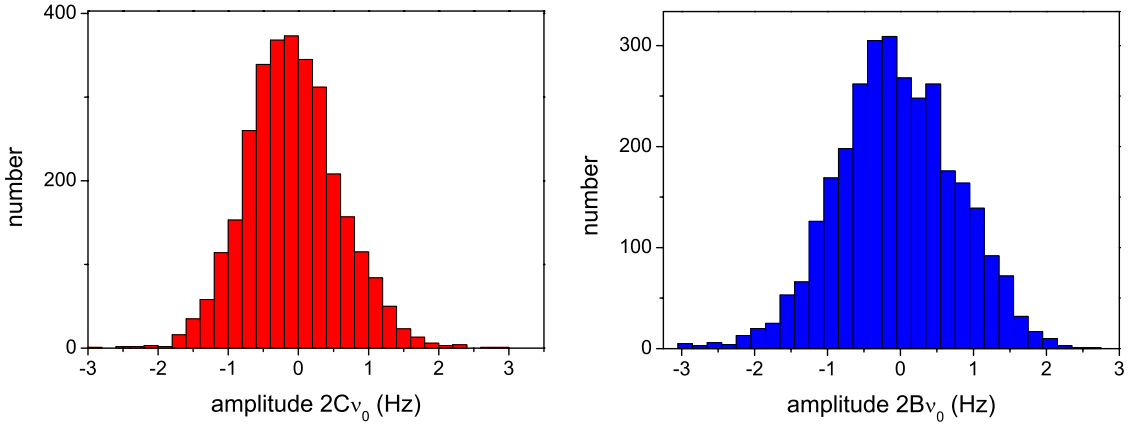

Fig. 11. Modulation amplitudes for a set of runs totalling 3050 rotations. Means and standard deviations of the data are (−0.08 and 0.66 Hz) for $2Cv_0$ and (−0.05 and 0.82 Hz) for $2Bv_0$.

mined to be, respectively, below 1×10^{-15} and 9×10^{-15} in absolute value, including their 1σ errors [8]. Assuming those parameters to be zero, we can obtain

$$(\tilde{\kappa}_{e^-})^{ZZ} = 4\langle 2C\rangle/(3\sin^2\chi) = -0.98 \times 10^{-15}.$$

Here χ is the colatitude of the laboratory. The statistical error is negligible compared to the systematic error, which at present can only be estimated. One conservative estimate is the standard deviation of the data, amounting to 8.0×10^{-15}. In other work [6,8] it has been assumed that

any systematics averages out if the data set is long enough. The data was subdivided in subsets lasting from one to several days and as uncertainty the standard deviation of the mean of the subset results was taken. Applying this procedure to our data, we obtain the standard error of the subset mean $\Delta(2Cv_0) = 0.094$ Hz. Considering that, e.g. the histogram of the $2Bv_0$ values shows deviations from a Gaussian we conservatively take as total uncertainty a value twice as large, corresponding to $\Delta(\tilde{\kappa}_{e^-})^{ZZ} = 2.3 \times 10^{-15}$.

4. Summary

We have described the implementation and characterization results of a novel apparatus aiming for a significantly improved test of the isotropy of the speed of light. The noise floor of the apparatus was determined, and different systematic effects were investigated.

Neglecting systematic effects caused by rotation of the system and assuming long-term stability, we estimate that continuous data acquisition time of 1 month would lead to a detection sensitivity of 5×10^{-18} for the modulation amplitude $2C$. In the future, the use of a larger ULE cavity spacer and larger cavity mirrors, resulting in a larger spot size, might allow reducing the thermal noise limit and further improve the fundamental detection sensitivity of the system.

In case of rotation of the setup we observed systematic effects which we estimated as $\Delta(2Cv_0) \sim 0.2$ Hz, or 7×10^{-16} in relative units. Several effects probably contribute and an extended investigation is required to identify them.

At this level of systematics we have established a value

$$(\tilde{\kappa}_{e^-})^{ZZ} = (-1.0 \pm 2.3) \times 10^{-15},$$

assuming all other SME coefficients vanish. The estimated error of this quantity is about a factor 10 below that of our previous experiment [5] and also significantly below the statistical errors quoted in the results of [6,8], respectively.

In the near future, our apparatus will be upgraded with a high-performance air-bearing rotation table and we expect to be able to reduce the systematic effects further, allowing an improved test of the isotropy of light propagation.

Acknowledgement

This work was supported by the German Science Foundation. Ch. Eisele gratefully acknowledges a fellowship from the Düsseldorf Entrepreneurs Foundation (Gründerstiftung).

References

[1] A.A. Michelson, E.W. Morley, Am. J. Sci. 34 (1887) 333.
[2] A. Brillet, J.L. Hall, Phys. Rev. Lett. 42 (1979) 549.
[3] H. Müller, S. Hermann, C. Braxmaier, S. Schiller, A. Peters, Phys. Rev. Lett. 91 (2003) 020401.
[4] P. Wolf, M.E. Tobar, S. Bize, A. Clairon, A.N. Luiten, G. Santarelli, Gen. Relat. Gravit. 36 (2004) 2351.
[5] P. Antonini, M. Okhapkin, E. Göklü, S. Schiller, Phys. Rev. A 71 (2005) 050101(R);
S. Schiller, P. Antonini, M. Okhapkin, Lecture Notes in Physics, vol. 702, Springer, 2006, p. 401.
[6] S. Hermann, A. Senger, E. Kovalchuk, H. Müller, A. Peters, Phys. Rev. Lett. 95 (2005) 150401.
[7] P.L. Stanwix, M.E. Tobar, P. Wolf, M. Susli, C.R. Locke, E.N. Ivanov, J. Winterflood, F. van Kann, Phys. Rev. Lett. 95 (2005) 040404.
[8] P.L. Stanwix, M.E. Tobar, P. Wolf, C.R. Locke, E.N. Ivanov, Phys. Rev. D 74 (2006) 081101(R).
[9] R. Mansouri, R.U. Sexl, Gen. Relat. Gravit. 8 (1977) 809.
[10] D. Colladay, V.A. Kostelecký, Phys. Rev. D 55 (1997) 6760.
[11] D. Colladay, V.A. Kostelecký, Phys. Rev. D 58 (1998) 116002.
[12] V.A. Kostelecký, M. Mewes, Phys. Rev. D 66 (2002) 056005.
[13] V.A. Kostelecký, Phys. Rev. D 69 (2004) 105009.
[14] S. Schiller, Presented at 339th W.E. Heraus Seminar on Special Relativity, Potsdam 2005;
C. Lämmerzahl, H. Dittus, A. Peters, S. Schiller, Class. Quant. Gravit. 18 (2001) 2499.
[15] A.Yu. Nevsky, M. Eichenseer, J. von Zanthier, H. Walther, Opt. Commun. 210 (2002) 91.
[16] M.V. Okhapkin, M.N. Skvortsov, A.M. Belkin, N.L. Kvashnin, S.N. Bagayev, Opt. Commun. 203 (2002) 359.
[17] S. Seel, R. Storz, G. Ruoso, J. Mlynek, S. Schiller, Phys. Rev. Lett. 78 (1997) 4741.
[18] R. Storz, C. Braxmaier, K. Jäck, O. Pradl, S. Schiller, Opt. Lett. 23 (1998) 1031.
[19] K. Numata, A. Kemery, J. Camp, Phys. Rev. Lett. 93 (2004) 250602.